Research Journal of Recent Sciences _____ ISSN 2277-2502
Vol. **6(4),** 18-27, April **(2017)** *Res. J. Recent Sci.*

Scavenging of phenolic compounds from aqueous waste using magnetic nanoparticles activated carbon prepared from date seed

Rinku Jaiswal[1*], Shripal Singh[1] and Hemant Pande[2]
[1]CIMFR Nagpur Unit-II, 17/C-Telenkhedi area, Civil Lines, Nagpur-440001, MS, India
[2]Hislop College, Civil Lines, Nagpur, MS, India
rinku.jaiswal7777@gmail.com

Available online at: www.isca.in, www.isca.me
Received 14th January 2017, revised 11th March 2017, accepted 23rd March 2017

Abstract

Phenol and its derivatives constitute a group of pollutants that are present in industrial and domestic wastewater and carcinogenic in nature. Adsorption on Magnetic nanoparticles activated carbon (MNAC) has emerged an efficient and economically viable technology for removal of toxic phenolic compounds from domestic and industrial wastewater. In the present study activated carbon (AC) is prepared from date seed using KOH in a modified muffle furnace. The magnetic nanoparticles activated carbon (MNAC) is prepared by combining this activated carbon with magnetic nanoparticles developed by coprecipitation method. A variety of techniques such as N_2-BET surface area, SEM, FT-IR, XRD, TEM, pH pzc and VSM were used to characterize the structure, morphology and magnetic performance of MNAC. The N_2-BET surface area of the MNAC (894 m^2g^{-1}) is found lesser than the prepared AC (2298 m^2g^{-1}). A broad peak at $2\theta = 24^0$ in XRD of AC & MNAC indicates the presence of amorphous carbon. The TEM of MNAC shows iron oxide nanoparticles of size 5-20 nm. MNAC exhibits super magnetic properties under external magnetic field with saturation magnetization value 5.52 emu/g at room temperature. The adsorption of priority phenolic pollutants, namely phenol, p-nitrophenol, o-chlorophenol, o-methoxy phenol on activated carbon and magnetic nanoparticles activated carbon, was studied in a batch system at laboratory scale. The adsorption equilibrium isotherm data shows good linearity when plotted according to Langmuir, Freundlich and BET isotherm equations. The Langmuir Q^0 value, for AC & MNAC show the trend: OCP> PNP > OMP >P. Langmuir kinetic model best suits for determination of adsorption and desorption rate constants for these pollutants. The Pseudo-second order model fit better than Pseudo-first order model for the adsorption of organic pollutants onto AC and MNAC.

Keywords: Activated carbon, Iron oxide, Phenolic compound, Adsorption isotherm, Kinetic.

Introduction

Phenol and its derivatives constitute a group of pollutants that are present in industrial and household wastewater and harmful in nature. In order to accede the acrimonious environmental directions, many treatment technologies have been developed to remove these pollutants from household and industrial wastewaters. Out of many available wastewater treatment technologies, adsorption on activated carbon has been appeared one of the most suitable and economically viable technologies. There are several reports on adsorption of organic pollutants on activated carbon. Casta and Rodrigues studied the adsorption of phenol and p-nitrophenol from aqueous phase on GAC[1] and interpreted experimental data by IAS theory formulated by Radke and Prausnitz[2]. Chern and Chien investigated competitive adsorption of benzoic acid and p- nitrophenol onto activated carbon and concluded that GAC has higher affinity to PNP than Benzoic acid[3]. Fritz and Schlunder proposed a general empirical equation for calculating the adsorption equillibria of organic solutes in solution and successfully tested for aqueous solution of phenol and p-nitropheno[4]. Srivastava and Tyagi Studied competitive of substituted phenols by activated carbon developed fertilizer waste slurry[5]. Khan et al presented adsorption of phenol-based organic pollutants on activated carbon from multi-component dilute aqueous solutions[6].

Activated carbon is a versatile material due to its wide applications in gas separation, wastewater treatment, as catalyst support, liquid purification, hydrogen gas storage, material for double layer capicitor and medicinal uses. It is a non-graphitic and non-graphitizable carbon having very high surface area ranging from 600-1200 m^2/g and pore volume 0.5-1.2cm^3/g[7]. Magnetic nanoparticles activated carbon is the formation of composite materials prepared by adding of appropriate inorganic iron oxide nanoparticles in the pores of Activated carbons. Iron oxide nanoparticles are iron oxide particles with diameters between about 1 and 100 nm. MNAC which can easily separated from complex system to a desired place using external magnetic field.

Magnetic nanoparticles have accomplish appropriate consideration in waste water treatment[8], established on their advantage such as accessible dissociation, simple handling process, affectionate application quality and simple accurately functional conversions.

The present work is an attempt to prepare low cost magnetic nanoparticles activated carbon (MNAC) composite from date seeds for the removal of organic pollutants from aqueous wastes.

Materials and methods

All chemicals used were analytical grade obtained from Merck, India. The date seeds were collected from the local market of Nagpur City (India) and crushed to -5 to +1 mm size. This material is washed with distilled water to remove any dirt and dried.

Preparation of activated carbon: The sized and dried date seeds were impregnated with KOH in different ratios and kept undisturbed for 24 hours. Impregnated material was carbonized in a modified muffle furnace with N_2 gas inflow arrangement at 500-900^{0}C for 1-3 hours. After carbonization, the sample was de-ashed with 5N HCl followed by washing with distilled water to remove any acid present in the sample. The pH of the carbon washings was checked with a portable pH meter (PCTestr 35-Oakton 35425-00-Singapore). The washed carbon was dried at 108±2^{0}C in a moisture oven for 24 hours and kept in a desiccator.

Preparation of Magnetic nanoparticles activated carbon (MNAC): The magnetic nanoparticles activated carbon (MNAC) was made by a chemical co-precipitation method. Synthesis of iron oxide magnetic nanoparticles was carried out by co-precipitation method of Fe^{2+} and Fe^{3+} salts under the presence of Nitrogen gas.

$$Fe^{2+} + 2Fe^{3+} + 8OH^- \rightarrow Fe_3O_4 + 4H_2O \quad (1)$$

To prepare MNAC, Fe_3O_4 magnetic nanoparticles were combined with aqueous suspension of activated carbon. The sample was reacted in a modified furnace at 800°C for 3h under nitrogen gas atmosphere. The synthesized MNAC was washed with deionised water for four times and then dried at a 100°C in a moisture oven and kept in a desiccator for use.

Method for adsorption isotherm, kinetics study: To evaluate the adsorption isotherm data, adsorbate solutions of different concentrations were prepared by diluting the stock solution with calculated volume of water. The initial concentration was determined by ultraviolet-visible spectrophotometer (Lambda 35 model, Perkin Elmer UV/VIS spectrophotometer).

For kinetics study, the experimental unit was a cylindrical batch reactor of 7L capacity and made of teflon and was fitted with baffles was used. 3g of weighed AC and MNAC were introduced into 3L of phenolic solution of known concentration with constant stirring at 30°C. The adsorbate was withdrawn after regular interval and the concentration was examined by using Ultraviolet-visible spectrophotometer.

Characterization AC and MNAC: Iodine number, N_2-BET Surface area and pore volume: To determine micro pores structure of AC and MNAC, iodine number was determined as per ASTM D4607-94(1999). The iodine number of AC; 1946 mg g^{-1} is more than that of MNAC; 843 mg g^{-1}. The surface area and pore volume of prepared AC and MNAC were determined by SMARTSORB 92/93 N_2- BET surface area analyzer. This instrument is based on Brunaur, Emmet and Teller (BET) theory. N_2BET and pore volume of AC are 2298 m^2 g^{-1} and 1.1030 cm^3 g^{-1} and MNAC are 894 m^2 g^{-1} and 0.3342 cm^3 g^{-1} respectively. It reveals that magnetization processes affected the Iodine value, surface area and the pore volume. Micro porosity development is substantially reduced in MNAC. The lesser surface area of the MNAC is due to partially filling of pores of AC with Fe_3O_4 nanoparticles.

Scanning electron microscopy: The surface morphology of AC and MNAC were studied by scanning electron microscopy (SEM) with a JEOL JSM-6380 model Scanning Electron Microscope. The SEM micrographs of AC and MNAC are shown in Figure-1 and Figure-2 respectively. A porous, spongy texture in the case of AC can be seen in Figure-1. The micrograph (Figure-2) shows the morphological changes due to iron oxide impregnation on the surface of the carbon matrix with mass ratio of 1/2 respectively. After iron oxide impregnation, the surface texture shows less spongy structure than AC.

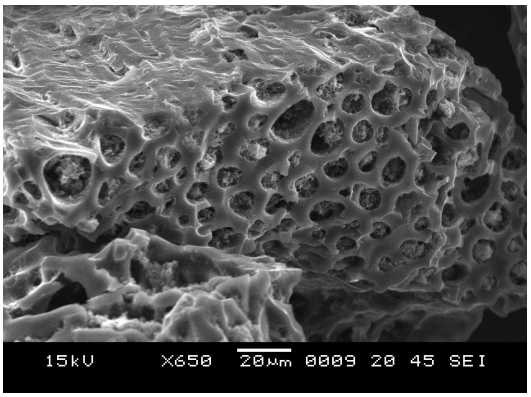

Figure-1: SEM of DSAC

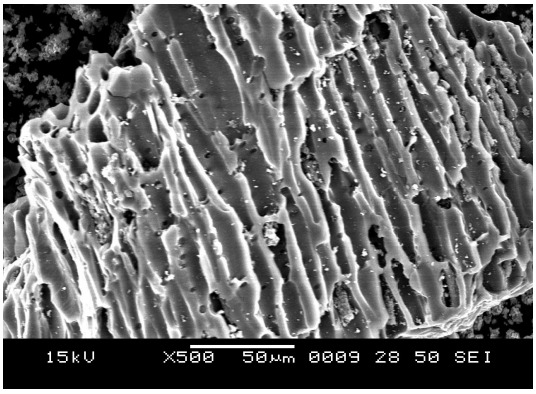

Figure-2: SEM of MNAC.

Transmission electron microscopy: The size and shape of nanoparticles of MNAC were observed by Transmission electron microscopy (TEM) and high resolution TEM (HRTEM) on JEOL JEM-2010F.TEM micrographs for the prepared MNAC and are shown in Figure-3 (a-b). From these micrographs it is observed that the particle size of the nanoparticles lie in the range of 5-20 nm. The particles formed tend to cluster as they are magnetic in nature. Recording of higher resolution images of the carbon might be quite difficult owing to its highly disordered structure[9]. The primary carbon particles are interconnected with each other to form networks. MNAC primary particles exhibited a rounded cubic shape with an almost homogenous in size distribution. The iron-oxide nanoparticles were well dispersed.

FT-IR spectroscopic analysis: To resolve the functional groups present and its wave numbers, FT-IR of AC and MNAC were carried out by using Fourier transform infrared spectrophotometer (FT-IR) (Perkin Elmer, PE-RXI) in the range of 450-4000cm^{-1}. In FT-IR of AC, Figure-4(a), the predominant presence of free phenolic –OH stretch vibration around 3148 cm^{-1}is observed. The band around 2372cm^{-1} is due to carboxylic O-H stretch vibrations. The band around 1559cm^{-1} is observed due to the presence of carboxylate group COO^{-}. The peak at 1401cm^{-1} is due to C-N vibrations of aliphatic amine. The spectra around 1000cm^{-} and below is marked by the noisy spectrum that may due to the presence of mineral matter. In FT-IR spectra of MNAC Figure-4 (b) a broad and strong band at 3747-3272 cm^{-1} is due to the stretching vibrations of –OH, which is assigned to OH^{-} absorbed by Fe_3O_4 nanopartcles. MNAC exhibits a carbonyl peak at 1110 cm^{-1}, and peaks at 690 cm^{-1} and 587 cm^{-1} which are attributed to the Fe-O bond vibration of Fe_3O_4 compatible with the presence of iron oxides in the sample[10].

X-ray diffraction: The X-ray diffraction (XRD) patterns of magnetic activated carbon and date seed activated carbon were obtained on a powder X-ray diffraction system from analytical model XPERT-PRO diffractometer. Powder X-ray diffraction patterns are presented in Figure-5(a) and (b). Only one broad peak centered at about 2θ = 24° was observed in AC confirming the amorphous nature of the carbon. When studying activated at about such a scattering angle was associated with the diffraction. It has been used to estimate the stacking number of graphene sheets (Lc or N)[11]. The X-ray diffraction patterns for MNAC display a number of sharp peaks which are compatible with the presence of $Fe(OH)_2$ and $Fe(OH)_3$ (peaks at 2θ = 38.11^0,40.18^0 and 61.90^0) and of Fe_2O_3 (peaks at 2θ = 49.58^0, 54.16^0 and 64.93^0). This illustrates that domain of iron species exist which is crystalline in the MNAC sample.

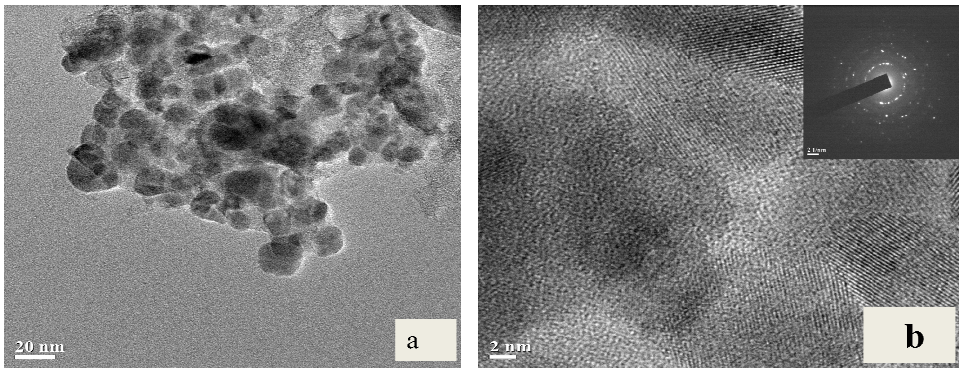

Figure-3: (a) TEM of MNAC & (b) HRTEM of MNAC.

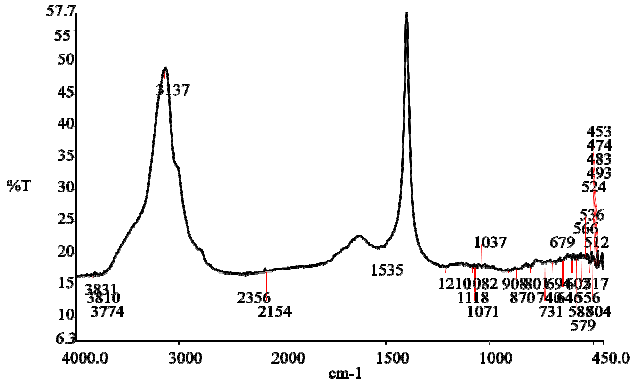

Figure-4: (a) FTIR of DSAC.

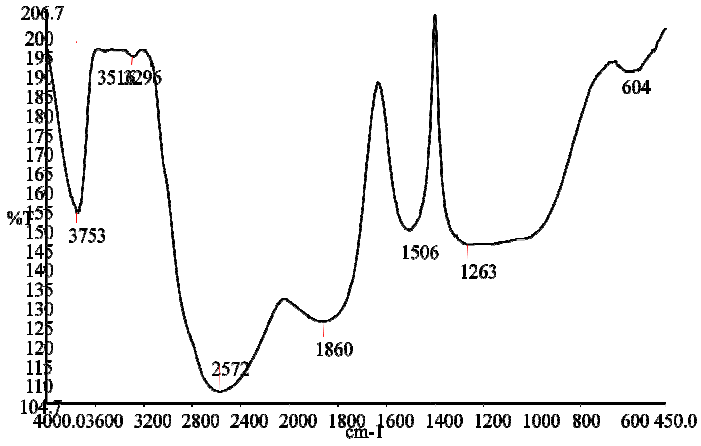

Figure-4: (b) FTIR of MNAC.

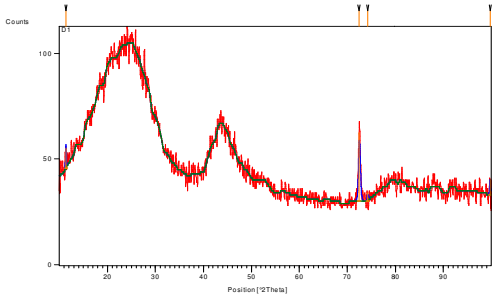

Figure-5(a): XRD of DSAC.

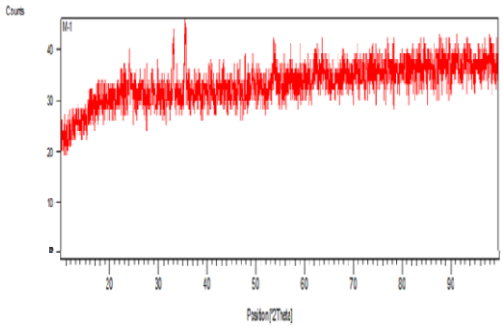

Figure-5(b): XRD of MNAC.

Vibrating sample magnetometer: The hysteresis measurement was carried out using Lakeshore vibrating sample magnetometer (VSM) 7410 at room temperature. The suitability of ferromagnetic materials for application depends on characteristics shown by their hysteresis loops[12] obtained from plots of magnetization (M) against the field strengths. The saturation magnetization of magnetic activated carbon is 5.52 emu/g at room temperature as shown in (Figure-6 (a)). However, MNAC has a good response under the additional permanent magnetization (Figure-6(b)), which made the solid and liquid phases separate quickly.

Results and discussion

Adsorption Isotherms: In order to study the dominant adsorption mechanism and to compute various adsorption parameters three adsorption models, namely Langmuir, Freundlich and BET were used.

The Langmuir isotherm: The Langmuir adsorption isotherm has been used by many authors for the adsorption of inorganic and organic substances. The Langmuir adsorption model[13] is based on the assumption that maximum adsorption corresponds to a saturated monolayer of solute molecules on the adsorbent surface, with no lateral interaction between the sorbed molecules. The linear form of the Langmuir isotherm is given by the following equation:

$$1/Q_e = (1/Q_0) + (1/Q_0 b) \times 1/C_e \quad (2)$$

Where: Q_e is the maximum amount of the phenolic compound adsorbed per unit weight of the adsorbent at equilibrium, Q_0 is the monolayer capacity of adsorbent, C_e is the concentration of adsorbate at equilibrium, and b is a Langmuir constant. Langmuir parameters Q_0 and b were calculated from the slope and intercept of the linear plots of $1/Q_e$ vs. $1/C_e$ as given in Figure-7(a) and Figure-7(b).

The values of Q_0 and b for activated carbon and magnetic nanoparticle activated carbon are calculated from the slope and intercept of the straight line and summarised in Table-1. The results show that magnetic nanoparticle activated carbon has a lower adsorption capacity than activated carbon. This is due to the covering of surface of activated carbon with Fe_2O_3 as evident from the decrease in the N_2-BET surface area and SEM.

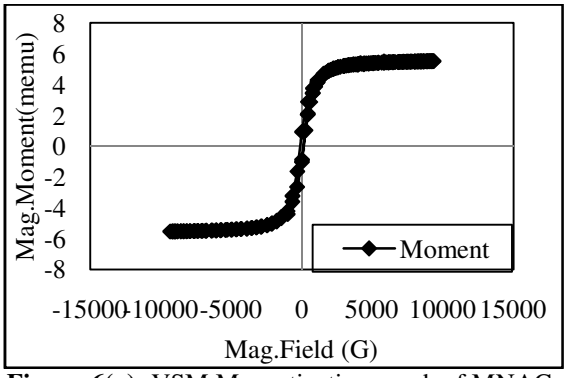

Figure-6(a): VSM Magnetization graph of MNAC.

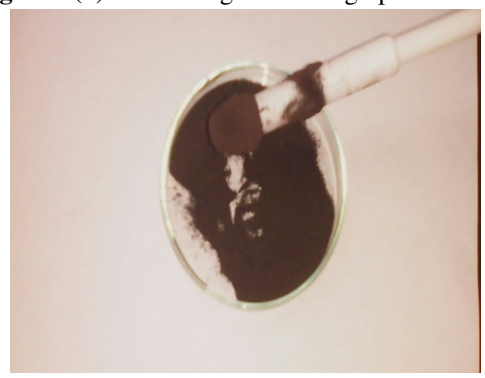

Figure-6(b): MNAC attracted by magnetic retriever.

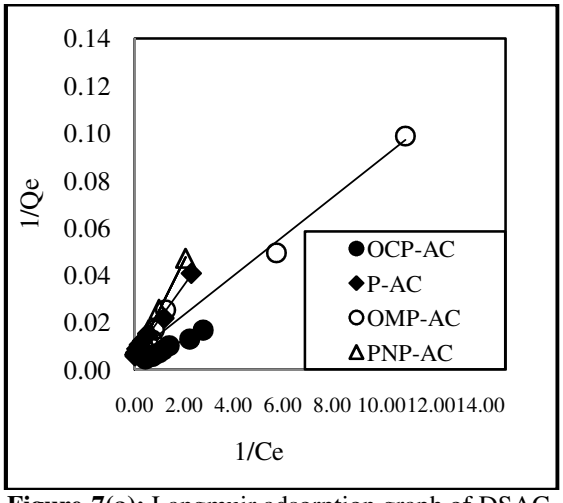

Figure-7(a): Langmuir adsorption graph of DSAC.

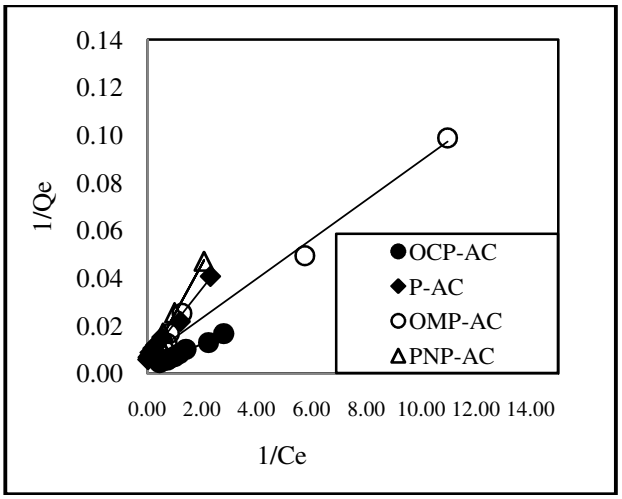

Figure-7(b): Langmuir adsorption graph of MNAC.

Freundlich isotherm: The adsorption data for phenol was also evaluated by the Freundlich isotherm. The Freundlich isotherm[14] is an empirical equation employed to describe heterogeneous systems. The linear form of Freundlich adsorption model is as follows:

$$\text{Log } (Q_e) = \text{Log}K_f + 1/n \text{ Log } (C_e) \quad (3)$$

Where: Ce is the equilibrium concentration (mgL–1), Q_e is the amount adsorbed (mg g–1). K_f and n are Freundlich constants related to adsorption capacity and adsorption intensity respectively. Log Q_e was plotted against Log C_e for the equilibrium data of phenol and shown in Figure-8(a) and Figure-8(b). The Freundlich constants K_f and n for activated carbon and magnetic activated carbon were calculated from the slope and intercept of the plot and given in Table. The correlation coefficients for both adsorbents in Table 1 are low and therefore the values of K and n cannot be compared. The best fit was observed with Langmuir and BET models as the correlation coefficient for these models are more than 0.98.

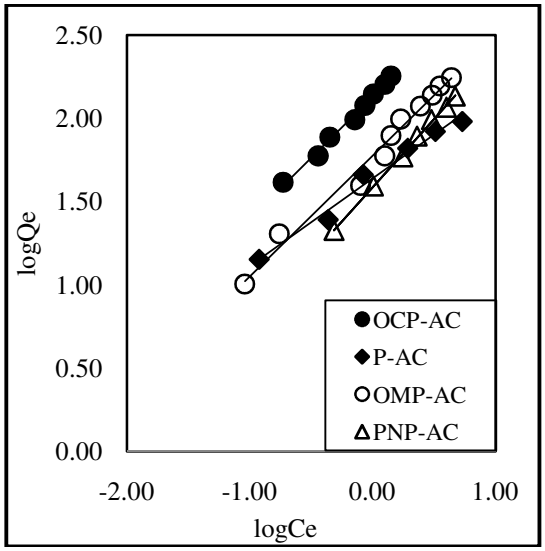

Figure-8(a): Freundlich adsorption graph of DSAC.

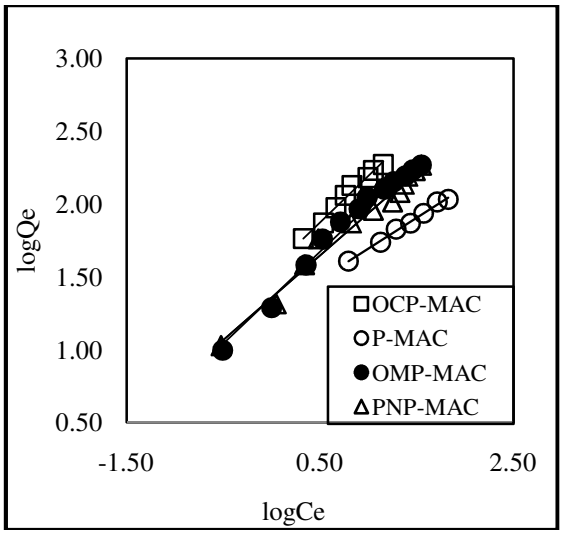

Figure-8(b): Freundlich adsorption graph of MNAC.

The BET adsorption isotherm: The BET adsorption isotherm explains the physical adsorption of gas/solid molecules on a solid surface and serves as the basis for an important analysis technique for the measurement of the specific surface area of a material.

The BET adsorption model can be derived similar to the Langmuir adsorption model, but by considering multilayered gas/solid molecule adsorption, where it is not required for a layer to be completed before an upper layer formation starts.

The Langmuir adsorption isotherm is usually better for chemisorptions and the BET adsorption isotherm works better for physisorption for non-micro porous surfaces. The BET adsorption equation can represented as:

$$C_e/Q_e\ (C_s-C_e) = 1/Q_0z + (z-1/Q_0z)*C_e/C_s \quad (4)$$

Where: C_e, Q_e, Q_0, have the same meaning as in Langmuir model, C_s is the saturated concentration of the adsorbate and z is BET constant. BET parameters Q_0 and z were calculated from the graph plotted between C_e/C_s vs. C_e/Q_e (C_s-C_e) in Figure-9(a) and 9(b). The values of Q_0 and z for activated carbon and magnetic activated carbon calculated from the slope and intercept of the straight line are given in Table-1. The Q_0 value for MNAC is more than AC. The reason is same as given in Langmuir adsorption model.

A glance at the Q^0 values, for AC and MNAC the adsorbates shows the trend: OCP > PNP > OMP > P. The Q^0 values of AC and MNAC shows that the OCP is better extent as compared to OMP and Phenol. The Q^0 values show that derivatives of phenols are better adsorption capacity than phenol.

The reduction in Q^0 values of magnetic activated carbon can be attributed to reduction in surface area due to iron oxide impregnation.

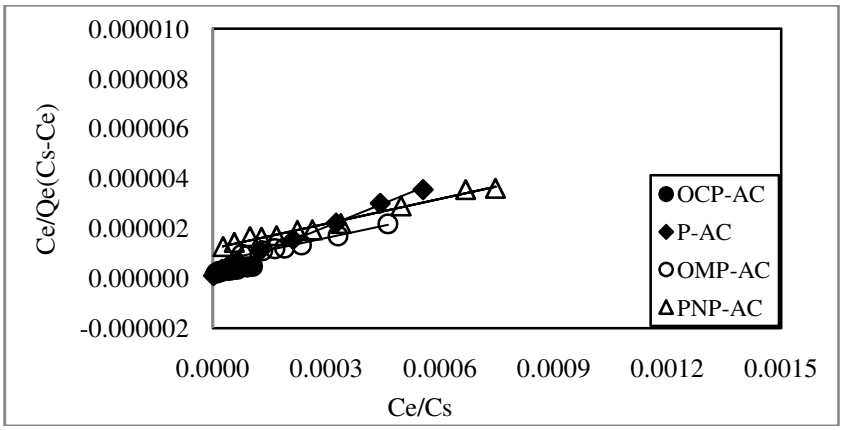

Figure-9(a): BET adsorption graph of DSAC.

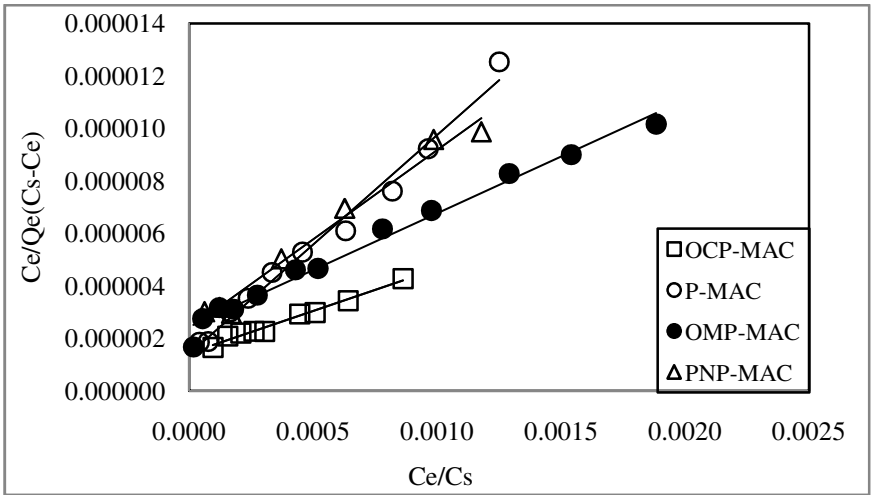

Figure-9(b): BET adsorption graph of MNAC.

Kinetic study for AC and MNAC: Modelling of kinetic data is important for the industrial application of the adsorption process, because it gives information that can be used to compare different adsorbents under different operating conditions for removing pollutants wastewater.

The kinetic models used to investigate and describe the adsorption of organic pollutants are the Langmuir kinetics, pseudo-first order, pseudo-second order, and intra particular diffusion models.

Langmuir kinetics model: In the present study, a simplified interpretation of the kinetics data based on Langmuir theory[15] is used. Langmuir theory assumes that the rate of adsorption is proportional to the product of adsorbate concentration in the fluid phase and the fraction of the vacant adsorbent surface. The fraction of the surface covered by the adsorbate, q, will be the proportional to the decrease in fluid phase adsorbate concentration, thus

$$\frac{dq}{dt} = k_a C (1-q) - k_d q \quad (6)$$

and

$$q = (C_o - C_t) \quad (7)$$

Where: k_a and k_d are adsorption and desorption rate constants. C_o, C and C_e are the fluid phase adsorbate concentration at zero, time t and at equilibrium respectively, f is a constant. Substituting equation (6) in equation (7) and solving the resultant equation by applying the concept of steady state gives the final rate expression:

$$\ln [(C_t-C_e)/(C_t + a)] = -K C_e t + \ln [(C_o-C_e) /(C_o + a)] \quad (8)$$

Where: $a = (C_o/ KC_e)$ and $K= k_a / k_d$, the Langmuir constant.

The adsorption and desorption rate constants were thus evaluated by plotting $\ln [(C_t-C_e) / (C_t + a)]$ against t. Figure-9(a) and 9(b) and Table-2 reports the value of adsorption rate constants for organic pollutants on activated carbon and MNAC.

The adsorption rate constant trend for the systems studied is; OCP > PNP > OMP > P. From the above K_a and K_d data it can be inferred that the rate of adsorption (K_a) is very high than the rate of desorption (K_d) for the adsorbates on AC and MNAC.

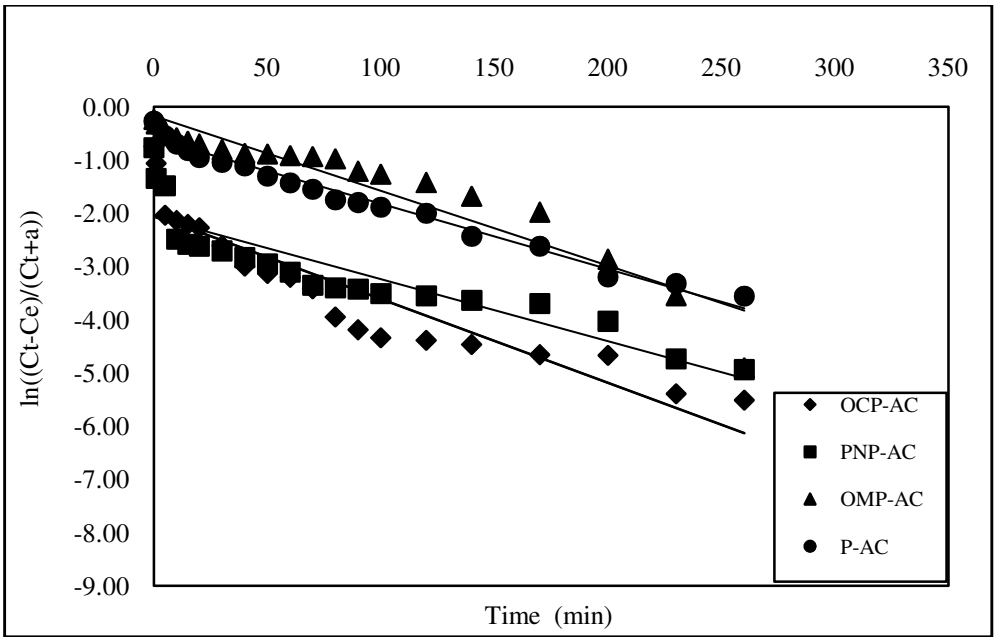

Figure-9(a): Langmuir kinetic graph of DSAC.

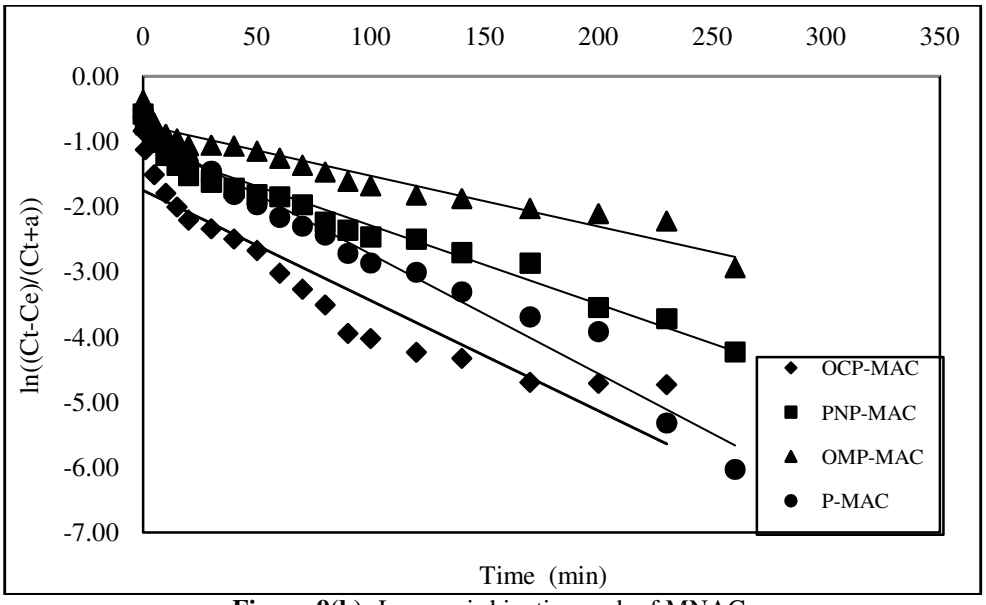

Figure-9(b): Langmuir kinetic graph of MNAC.

Pseudo-second order: As Pseudo-first order equation is not followed in the present study, Pseudo-second order was analysed. A reaction involving pseudo-second-order kinetics requires that the reaction rate is directly proportional to the number of active sites on the adsorbent surface.

The linearized form of the pseudo second-order equation is expressed as follows:

$$t / q_t = 1 / k_2 q_e^2 + t / q_e \quad (9)$$

$$h = k_2 q_e^2 \quad (10)$$

q_t is the amount of organic pollutants adsorbed at time t (mg/g), q_e is the amount of organic pollutants adsorbed at equilibrium (mg/g), h is the initial sorption rate (mg/g.min). The value q_e (1/slope), k_2 (slope^2/intercept) and h (1/intercept) can be calculated from the plots of t/q_t versus t. The linear plots of pseudo-second order model of organic pollutants are presented in Figure-10 and Figure-11.

The pseudo second order model showed the best fit to the experimental data related to the adsorption of organic pollutants onto activated carbon and magnetic nanoparticle activated carbon with the highest squared correlation coefficient (0.999).

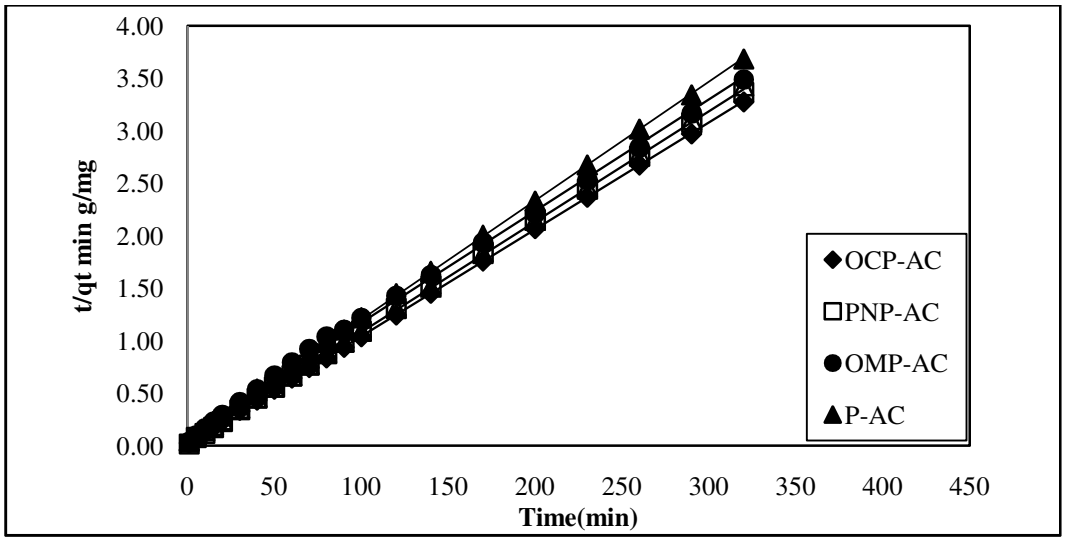

Figure-10: Pseudo second order graph of DSAC.

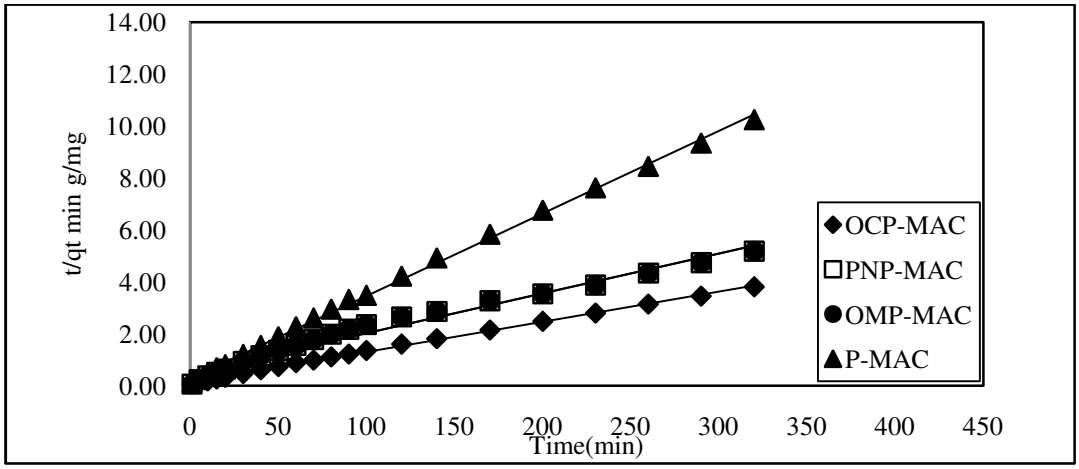

Figure-11: Pseudo second order graph of MNAC.

Table-1: Adsorption isotherm constants for organic pollutants on DSAC and MNAC.

Sr. No.	Adsorbent	Adsorbate	Langmuir constant		Freundlich constant		BET constant	
			Q^0	b	K_f	1/n	Q^0	Z
1	DSAC	OCP	500	0.4	134.58	0.733	500	9999
		PNP	250	0.1904	38.459	0.818	333	2999
		OMP	166	0.75	13.061	0.725	333	4999
		P	125	0.5714	35.974	0.646	142	34999
2	MNAC	OCP	333	0.1	35.80	0.640	333	29999
		PNP	166	0.1333	22.698	0.579	166	2999
		OMP	125	0.2758	22.750	0.631	250	1999
		P	90	0.1047	15.523	0.447	125	7999

Table-2: Kinetics constants for organic pollutants on DSAC and MNAC.

Sr.No.	Adsorbent	Adsorbates							
		OCP		PNP		OMP		P	
		K_a	K_d	K_a	K_d	K_a	K_d	K_a	K_d
1	DSAC	915	0.0177	304.1	0.0114	224.2	0.0024	80.64	0.0015
2	MNAC	228	0.9776	123.9	0.0066	54.69	0.0016	47.57	0.0048

Conclusion

Date seed activated carbon (AC) and magnetic nanoparticles activated carbon (MNAC) were prepared, characterised and evaluated for removal of organic pollutants-OCP, PNP, OMP, and P from aqueous waste. The characterisation of date seeds and prepared activated carbon show that the date seeds are potential raw material to prepare activated carbon. SEM of AC shows presence of different size pores, crackes and crevices while SEM of MNAC morphological changes due to iron oxide impregnation on the surface of the carbon matrix. FT-IR Spectrum of AC and MNAC show the presence of various surface groups with predominant presence of phenolic –OH. The other surface groups present are carboxylic, carbonyl and aliphatic amines. The peaks at 691cm^{-1} and 558cm^{-1} are attributed to Fe-O bond vibration of Fe_3O_4 compatible with the presence of iron oxides in the sample. XRD analysis of AC shows only one broad peak at about $2\theta = 24^0$ which confirms the amorphous nature of the carbon. The TEM of MNAC shows Fe_3O_4 nanoparticles of size 5-20 nm. Fe_3O_4 nanoparticles with a cubic structure are clearly visible in the micrographs.VSM analysis of MNAC shows 5.52 emu/g magnetic strength at room temperature.

The adsorption capacity of iron oxide loaded composite adsorption is significantly decrease with an increase in the iron oxide loading. The reduction in adsorption capacity of MNAC can be attributed to the reduced porosity due to iron oxide impregnation. Langmuir kinetic model best suits for determination of adsorption and desorption rate constants for organic pollutants. The Pseudo-second order model fit better than Pseudo-first order model for the adsorption of organic pollutants onto activated carbon and magnetic nanoparticle activated carbon with the highest squared correlation coefficient (0.999).

References

1. Singh Shripal and Yenkie Mahesh K.N. (2006). Scavenging of Priority Organic Pollutants from Aqueous Waste using Granular Activated Carbon. *Journal of the Chinese Chemical Society*, 53(2), 325-334.

2. Radke C.J. and Prausnitz J.M.J. (1972). Ind Eng Chem Fundam. 11, 445.

3. Chern J.M. and Chien Y.W. (2003). Competitive adsorption of benzoic acid and p-nitrophenol onto activated carbon: isotherm and breakthrough curves. *Water Res.,* 37(10), 2347-2356.

4. Fritz W. and Schlünder E.U. (1981). Competitive adsorption of two dissolved organics onto activated carbon. Pt. 1: adsorption equilibria *Chemical Engineering Science*, 36(4), 721-730.

5. Srivastava S.K. and Tyagi R. (1995). Competitive adsorption of substituted phenols by activated carbon developed from the fertilizer waste slurry. *J. Wat. Res*., 29(2), 483-488.

6. Khan A.R., Al-Bahri T.A. and Al-Haddad A. (1997). Adsorption of phenol based organic pollutants on activated carbon from multi-component dilute aqueous solutions. *J. Water Res*., 31(8), 2102-2112.

7. Chilton N., Losso J.N., Marshall Wayne E. and Rao R.M. (2002). Physical and chemical properties of selected agricultural by product-based activated carbons and their ability to adsorb geomin. *Bioresource technology*, 84(2), 177-185.

8. Yavuz Cafer T., Mayo J.T., Yu William W., Prakash Arjun, Falkner Joshua C., Yean Sujin, Cong Lili, Shipley Heather J., Kan Amy, Tomson Mason, Natelson Douglas and Colvin Vicki L. (2006). Low field magnetic separation of monodispese Fe_3O_4 nanocrystals. *Science*, 314, 964-967.

9. Harris P.J.F., Liu Z. and Suenaga K. (2008). Imaging the atomic structure of activated carbon. *Journal of Physics*. Condensed Matter, 20(36), 362201-362206.

10. Marel H.W.v.d. and Beutelspacher H. (1976). Atlas of Infrared Spectroscopy of Clay Minerals and their Admixtures. Elsevier: Amsterdam.

11. Qu D. (2002). Studies of the activated carbons used in double-layer supercapacitors. *Journal of Power Sources*, 109(2), 403-411.

12. Jiles D. (1991). Introduction to Magnetism and Magnetic Materials. Chapman and Hall.

13. Lanowix IRVING (1918). The adsorption of gases on plane surface of glass, mica, and platinum. *J.Am. Chem. Soc*., 40, 1361-1402.

14. Freundlich HMF (1906). Over the adsorption in solution. *Phys. Chem*., 57, 385.

15. Todorovic M., Milonjic S.K., Comor J.J. and Gal I.J. (1989). In Radiation Protection Selected Topics; Dubrovnik Ed. Proceedings of the international radiation protection sysmposium. Yugoslavia, 654-659.